

See discussions, stats, and author profiles for this publication at: <https://www.researchgate.net/publication/265473574>

Polymer-Inorganic Coatings Containing Nanosized Sorbents Selective to Radionuclides. 1. Latex/Cobalt Hexacyanoferrate(II) Composites for Cesium Fixation

ARTICLE *in* ACS APPLIED MATERIALS & INTERFACES · SEPTEMBER 2014

Impact Factor: 6.72 · DOI: 10.1021/am5039196 · Source: PubMed

CITATIONS

3

READS

50

7 AUTHORS, INCLUDING:



[Svetlana Yu. Bratskaya](#)

Russian Academy of Sciences

78 PUBLICATIONS 717 CITATIONS

[SEE PROFILE](#)



[Alla Synytska](#)

Leibniz Institute of Polymer Research Dresden

64 PUBLICATIONS 987 CITATIONS

[SEE PROFILE](#)



[Valentin. A. Avramenko](#)

Russian Academy of Sciences

69 PUBLICATIONS 250 CITATIONS

[SEE PROFILE](#)

¹ Polymer-Inorganic Coatings Containing Nanosized Sorbents ² Selective to Radionuclides. 1. Latex/Cobalt Hexacyanoferrate(II) ³ Composites for Cesium Fixation

⁴ Svetlana Bratskaya,^{*,†} Anna Musyanovych,[‡] Veniamin Zhelezov,[†] Alla Synytska,[§] Dmitry Marinin,[†]
⁵ Frank Simon,[§] and Valentin Avramenko[†]

⁶ [†]Institute of Chemistry Far Eastern Branch of the Russian Academy of Sciences, Prosp.100-letiya Vladivostoka 159, 690022
⁷ Vladivostok, Russia

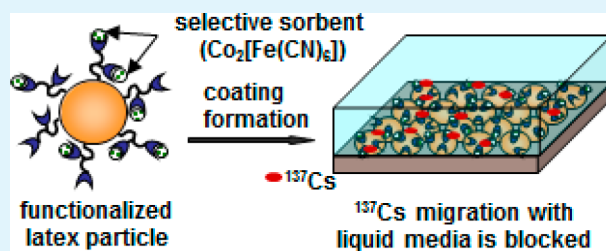
⁸ [‡]Max Planck Institute for Polymer Research, Ackermannweg 10, 55128 Mainz, Germany

⁹ [§]Leibniz-Institut für Polymerforschung Dresden e.V., Hohe Str. 6, 01069 Dresden, Germany

10 Supporting Information

ABSTRACT: Here we present a new approach to improve fixation of radionuclides on contaminated surfaces and eliminate their migration after nuclear accidents. The approach consists in fabrication of latex composite coatings, which combine properties of polymeric dust-suppressors preventing radionuclides migration with aerosols and selective inorganic sorbents blocking radionuclides leaching under contact with ground waters and atmospheric precipitates. Latex/cobalt hexacyanoferrate(II) (CoHCF) composites selective to cesium radionuclides were synthesized via “in situ” growth of CoHCF crystal on the surface of carboxylic or amino latexes using surface functional groups as ion-exchange centers for binding precursor ions Co^{2+} and $[\text{Fe}(\text{CN})_6]^{4-}$. Casting such composite dispersions with variable content of CoHCF on ^{137}Cs -contaminated sand has yielded protective coatings, which reduced cesium leaching to 0.4% compared to 70% leaching through original latex coatings. ^{137}Cs migration from the sand surface was efficiently minimized when the volume fraction of CoHCF in the composite film was as low as 0.46–1.7%.

KEYWORDS: ^{137}Cs , ferrocyanide, nanoparticles, radionuclide migration, soil, dust suppressor



1. INTRODUCTION

Presently, latex organic–inorganic composites keep gaining academic and industrial interest due to a wide range of possible applications and a beneficial combination of polymer properties with inorganic materials functionality.^{1–4} Inorganic nanoparticles can be incorporated into latexes during polymerization process,³ attached to the latex surface via electrostatic, hydrogen, or covalent bonding,² or “in situ” deposited on the latex surface.⁴ Such latex-inorganic composites have been already used for fabrication of coatings with high refractive index,³ improved hardness, water and stain resistance,^{2,5} self-sterilizing,⁶ and many others useful properties. To the best of our knowledge, latex coatings containing sorbents selective to radionuclides have not been previously reported, although hybrid polymer-inorganic thin films for selective adsorption and subsequent determination of radionuclides are known to the researchers.⁷ However, the interest in such materials is far beyond the narrow field of analytical preconcentration of radionuclides.

We have recently shown⁸ that nanoparticles of selective inorganic sorbents can be immobilized to latex particles and applied as “liquid” or colloidal stable sorbents for cesium recovery from solutions and contaminated solid materials.

Extending this approach to film-forming latexes can be used for fabrication of a new type of dust suppressing coatings, which would combine properties of protective polymer film and selective sorbent to increase efficiency of radionuclides fixation after nuclear accidents. Application of polymeric dust-suppressors became a general practice allowing radionuclides entrapment within thin polymer films on the surfaces contaminated after accidents on nuclear power plants (NPP), radiochemical plants, and weapon production facilities.⁹ Such measures help to securely eliminate migration of radionuclides with aerosols, but do not limit their mobility in solid phase under high humidity conditions due to solubility of the water-based polymer products¹⁰ or permeability of the latex coatings for small ions, including radionuclides.¹¹ This limits effective long-term open-air application of dust-suppressor, since under continuous exposure to atmospheric precipitations radionuclides can migrate from soil surface deep into the soil profiles.

Received: June 18, 2014

Accepted: September 9, 2014

Table 1. Characteristics of the Latexes

latex	composition	diameter	ζ potential	content of ionic groups			theoretical capacity for CoHCF mmol/g
		nm	mV	per NP	per nm ²	mmol/g of latex	
SL	polystyrene	162 ± 12	-8 ± 3	0	0	0.0236	0.0059
ASL-1	poly(styrene/AA)	166 ± 15	-23 ± 5	24 820	0.41	0.0974	0.0243
ASL-5		157 ± 25	-35 ± 8	81 159	1.59	0.184	0.0460
ASL-6		164 ± 9	-37 ± 6	225 762	3.37	0.144	0.3600
ASL-10		244 ± 47	-41 ± 9	409 998	3.50	0.0787	0.0190
BMMDS-0.3	poly(MMA/BA/DMVS/MAA)	142 ± 15	-30 ± 7	74 215	1.17	0.0336	0.0084
BMMDS-0.06		119 ± 13	-17 ± 5	18 652	0.31	0.133 ^a	0.1330
BMADS-0.3	poly(MMA/BA/DMVS/AEMA)	98 ± 15	+27 ± 5	41 267 ^a	0.98 ^a	0.0018 ^a	0.0018
BMADS-0.06		105 ± 12	+3 ± 1	13 455 ^a	0.37 ^a		

^arelated to content of amino groups, all other values are related to carboxylic groups.

Long-lived radionuclides released after the nuclear accidents not only pose direct serious health threats for inhabitants, but also exclude large territories from agricultural use for many years. Immediately after the contact with the soil surface, ¹³⁴Cs and ¹³⁷Cs radionuclides, which are of great concern due to their strong photon energies and long half-lives, are mainly localized at a depth of up to 5 cm.^{12,13} However, the rate of their downward migration in the soil is on average 1 cm/year¹⁴ and largely depends on the soil structure and composition. For example, the migration depth of cesium radionuclides in soils of Scotland exceeded 17 cm 23 years after the Chernobyl accident.¹⁵ Usually, the remediation activity starts several months after the accidents, and the amount of soil that must be removed afterward depends on how efficient were the first measures on prevention of radionuclides migration to deeper ground layers.¹⁶

The aim of the present work was to develop a new approach to improve fixation of radionuclides on contaminated surface, including soils and grounds, and prevent their migration under high humidity conditions. The approach is based on application of recently reported⁸ type of the latex composites containing inorganic selective sorbents, for example, cobalt hexacyanoferrate(II) selective to cesium ions,¹⁷ to form on contaminated surfaces composite dust-suppressing coatings minimizing cesium leaching to the environment.

2. EXPERIMENTAL SECTION

2.1. Chemicals and Reagents. Styrene (St) purchased from Merck and butyl acrylate (BA), methyl methacrylate (MMA), methacrylic acid (MAA), and acrylic acid (AA) purchased from Aldrich were distilled under reduced pressure and stored at -20 °C before use. Other reagents and solvents were used as received: diethoxy(methyl)vinyl silane (DMVS, Aldrich), aminoethyl methacrylate hydrochloride (AEMA, Aldrich), the hydrophobic initiator 2,2'-azobis(2-methylbutyronitrile) (V59, Wako-Chemicals), the hydrophobe hexadecane (Aldrich), a nonionic surfactant Lutensol AT50 - 100 poly(ethylene oxide)-hexadecyl ether with an ethylene oxide block length of about 50 units (BASF).

2.2. Latex Synthesis. All latexes used in the present work were synthesized by free radical copolymerization in the direct (oil in water) miniemulsion system.¹⁸ Briefly, 0.250 g of hexadecane, 100 mg of V59, and different amounts of monomers (except AEMA) were mixed together and added to the aqueous phase consisting of 24 g of demineralized water and 0.400 g of Lutensol AT50. For the synthesis of amino-functionalized latexes, AEMA was dissolved in the aqueous phase and then mixed with the oil (dispersed) phase. The amount of monomers used for the latex preparations is given in Supporting Information, Table S1.

Both phases were stirred together for 1 h at 1000 rpm for pre-emulsification, and the miniemulsion was prepared by ultrasonication

the mixture for 120 s at 90% intensity (Branson sonifier W450 Digital, 1/2" tip) at 0 °C to prevent polymerization. Afterward, the mixture was transferred into a round-bottom flask, which was then closed and placed into the oil bath at 72 °C. The reaction proceeded overnight under magnetic stirring at 600 rpm. After synthesis the latexes were purified from the surfactant excess by multiple centrifugation/ redispersion in demineralized water and characterized in terms of particle size, zeta potential, and functional groups density. The characteristics of the latexes are summarized in Table 1.

2.3. Composite and Coatings Preparation. To obtain composites, cobalt hexacyanoferrate (II) (CoHCF) was immobilized to carboxylic latexes by successive addition of aliquots of 0.01 M CoCl₂ and 0.005 M K₄[Fe(CN)₆] solutions to a latex dispersion with solid content of 0.5%, 2%, 5%, or 10% at pH = 5.2–5.4. When composites were prepared from amino latexes, reagents were added in the reversed sequence. Theoretical chemical composition of CoHCF in latex/ CoHCF composite was Co₂[Fe(CN)₆]; the actual chemical composition was determined as a difference between content of K, Na, Fe, and Co in stable dispersion and in supernatant after precipitation of latex/CoHCF composite by centrifugation at 14 000 rpm, 60 min. Metal contents were determined by atomic absorption spectroscopy using Solaar 6 M spectrometer (Thermo, USA). The CoHCF for all composites is given in Supporting Information, Table S2. For simplicity, taking into account small differences in composition of cobalt hexacyanoferrates, in all cases we will refer to a general notation, CoHCF. CoHCF content was varied from 2 × 10⁻⁵ to 0.06 mmol per 1 g of dry latex, and in all cases was calculated on the basis of Fe content. All composites were labeled as "latex name"/CoHCF, for example, ASL-1/CoHCF, which indicates composite prepared by immobilization of CoHCF in ASL-1 latex.

Coatings were fabricated by casting 0.2 mL of dispersions with the latex solid content of 2%, 5%, or 10% on the silicon wafer (for SEM measurements) or on double-sided adhesive tape covered with ¹³⁷Cs-spiked quartz sand (for ¹³⁷Cs leaching tests). All samples had geometrical surface area 5.29 cm². The volume fraction of CoHCF in composite coatings was calculated according to the following formula:

$$\phi = (C_{\text{CoHCF}} \cdot V_l \cdot C_l \cdot Mr_{\text{CoHCF}} / h_{\text{film}} \cdot S_{\text{film}} \cdot \rho_{\text{CoHCF}}) \cdot 100\%$$

where C_{CoHCF} is CoHCF content in composite, mol per 1g of the latex; Mr_{CoHCF} is molecular weight of CoHCF, C_l is latex solid content in composite dispersion, g/L; V_l is casted volume of the latex/CoHCF composite dispersion, L; h_{film} is coating thickness, cm; S_{film} is film area, cm²; ρ_{CoHCF} is CoHCF density (1.89 g/cm³).

2.4. Characterization of the Latex Particles and the Latex/ CoHCF Composites. The size and electrokinetic potential of the latex particles and the latex/CoHCF composites were determined in a 0.0001 M KCl solution at pH 6.4 and pH 5.4, respectively, by the photon correlation spectroscopy and laser Doppler electrophoresis methods on a Malvern ZetaSizer Nano ZS analyzer (typical correlation functions and size distributions for original latexes and composites are presented in Supporting Information, Figures S1 and S2). The content of -COOH and -NH₂ groups were determined by colloid titration using a particle charge detector PCD 02 (Mütek GmbH, Germany) in

165 combination with a 702 SM Titrino (Metrohm AG, Switzerland)
 166 automatic titrator.¹⁸
 167 The stability of latex/CoHCF composites was studied in 0.5% latex
 168 dispersions by quantifying the iron in aliquots of dispersion sampled
 169 from the surface of the liquid in a cylinder at fixed time intervals (the
 170 height of the liquid column was 5 cm). The stability of CoHCF
 171 dispersion prepared in distilled water was investigated for comparison.
 172 The iron content was determined by atomic absorption spectroscopy
 173 on a Solaar 6 M spectrometer (Thermo, USA).

174 **2.5. Characterization of the Latex and the Latex/CoHCF**
 175 **Composite Coatings.** *Scanning Electron Microscopy (SEM).* All
 176 SEM images illustrating morphology and topography of original latex
 177 and latex/CoHCF composite coatings were acquired on a NEON 40
 178 EsB Crossbeam scanning electron microscope from Carl Zeiss NTS
 179 GmbH, operating at 3 kV in the secondary electron (SE) mode. To
 180 enhance the electron density contrast, samples were coated with
 181 platinum (3.5 nm) using a Leica EM SCDS00 sputter coater. The
 182 coating thickness was determined from cross-section SEM images after
 183 drying for 24 h at room temperature.

184 *Transmission Electron Microscopy (TEM).* A drop of the latex/
 185 CoHCF composite dispersion containing 0.035 mmol of CoHCF per
 186 1 g of latex was placed on a TEM grid and dried under ambient
 187 conditions. Copper grids covered with a holey carbon film (200 mesh,
 188 Quantifoil R1.2/1.3) were used for the analysis (Quantifoil GmbH,
 189 Germany). TEM images were taken with a Libra 200 TEM (Carl Zeiss
 190 Microscopy, Germany), equipped with an FEG running at an
 191 acceleration voltage of 200 kV. The in-column energy filter with an
 192 energy window of 20 eV was used. The images were recorded on a 4k
 193 camera (TVIPS GmbH, Germany) in 2 × 2 binning mode and
 194 adjusted in contrast and brightness using iTEM software (Olympus,
 195 Japan).

196 X-ray powder diffraction analysis was carried out on a Dron-3
 197 multipurpose diffractometer on the coating fabricated by spreading 2
 198 mL of latex/CoHCF composite dispersion (latex content 2%, CoHCF
 199 content 0.035 mmol per 1 g of dry latex) on quartz crystal plate. The
 200 coating thickness was ~50 μm.

201 The wettability of latex and latex/CoHCF composite coatings was
 202 investigated using contact angle measurements. Advancing and
 203 receding water contact angles were measured by the sessile drop
 204 method using a conventional drop shape analysis technique (Krüss
 205 DSA 10, Hamburg, Germany). Deionized reagent grade water was
 206 used for contact angle measurements. All contact angle measurements
 207 were carried out at 24 ± 0.5 °C and relative humidity of 40 ± 3%,
 208 which were kept constant.

209 **2.6. ^{137}Cs Leaching Test.** Quartz sand (fraction 0.100–0.315
 210 mm) preliminarily cleaned with a 0.1 M HCl solution and thoroughly
 211 washed was used to imitate the contaminated solid surface. To spike
 212 sand with cesium radionuclides, it was wetted with a solution
 213 containing ^{137}Cs , left until dry, and averaged over the volume. The
 214 resulting γ -activity of the sand sample was ~2000 Bq/g.

215 To obtain reliably fixed monolayers of sand particles, 60–70 mg of
 216 the ^{137}Cs -spiked sand was homogeneously distributed over 5.29 cm²
 217 piece of a double-sided adhesive tape attached into a Petri dish. The
 218 initial γ -activity of each sample was measured. The coatings on sand
 219 surfaces were formed as described in Section 2.3 and dried for 24 h
 220 prior to ^{137}Cs leaching experiments. Then 5 mL of distilled water or
 221 NaCl solution was introduced into the Petri dish and left without
 222 shaking for 24 h (or for the fixed time from 10 min to 10 d when
 223 studying the kinetics of the process). The ^{137}Cs distribution between
 224 the leaching solution and the solid phase was monitored by measuring
 225 the residual γ -activity of the quartz sand. In addition, the γ -activity of
 226 the solution was measured to ensure better γ -activity control.

227 The γ -activity of the ^{137}Cs γ radiation was determined by the direct
 228 spectrometric method from the line $E\gamma = 662$ keV with the use of a
 229 Gamma 1C universal spectrometer (Aspekt Research and Production
 230 Center, Russia). The γ activity of the samples was measured taking
 231 into account the “dead time” of the equipment. The counting rates
 232 were not higher than 10 000 counts/s. The specific activity of ^{137}Cs γ
 233 radiation in a solution was measured in 5 mL volume. The activity of
 234 solid samples after leaching was measured directly in the Petri dish for

235 point geometry. The conversion factor (k) from the point radiation 236 source to a bulk sample (5 mL) was determined from the ratio of the 236
 ^{137}Cs counting rate in a drop of a radioactive solution to the counting 237 rate after dilution and was equal to 1.41. 238

The amount of ^{137}Cs leached from the sand surface was estimated 239 as 240

$$L = (A_{\text{leached}}/A_0) \cdot 100\%$$

where A_0 is initial total γ activity of the solid sample, A_{leached} is total γ 241 activity of the solid sample after leaching. When A_{leached} was 242 determined by analyzing γ activity of the solution (A_{solution}), it was 243 calculated as $A_{\text{leached}} = k \cdot A_{\text{solution}}$. The difference between 244 calculated using γ activity of solid phase and liquid phase was in the 245 range of 1–3%. 246

3. RESULTS AND DISCUSSION

247 **3.1. General Concept of Composite Coatings for Radionuclides Fixation on Contaminated Surface.** The 248 general concept of the suggested approach is illustrated in 249 Figure 1 and consists in fabrication of latex composite coatings 250 fl

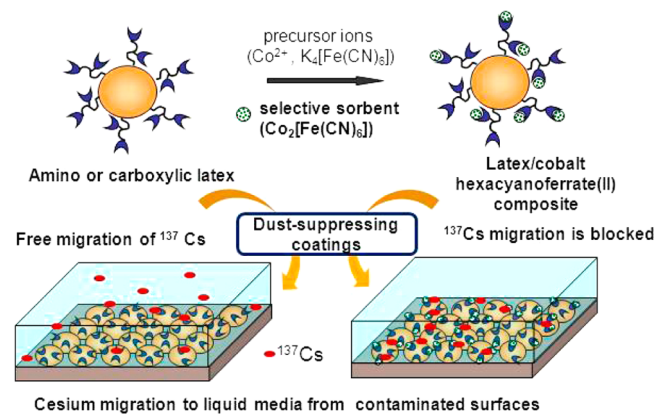


Figure 1. General concept of latex/cobalt hexacyanoferrate(II) (CoHCF) composites application for fabrication of coatings preventing cesium leaching and migration from contaminated surface.

containing nanosized sorbents with high selectivity to radio- 251 nuclides. We suggest that such coatings, combining dust- 252 suppressing properties of the latexes and sorption properties of 253 the inorganic materials, can be obtained by spraying or casting 254 dispersions of latex/sorbents composites on the contaminated 255 surface. The colloidal stable latex/sorbent composites can be 256 obtained either by electrostatic attachment of “ex situ” 257 synthesized sorbents nanoparticles to the latex surface or by 258 “in situ” growth of sorbent nanocrystals on the latex surface 259 using surface functional groups as ion-exchange centers for 260 binding precursor ions. One example of such composites 261 containing hexacyanoferrates(II) of several transition metals we 262 have demonstrated recently.⁸ The similar approach based on 263 anchoring of the metal precursor on the reactive organic groups 264 was used for fabrication of porous RuO₂@SiO₂ hybrids.⁹ 265

The main idea of the suggested approach here is based on 266 the assumption that the presence of the selective sorbent 267 nanoparticles in composite coatings can reduce permeability of 268 the latex film for target radionuclides and significantly decrease 269 radionuclides migration rate under the contact with atmos- 270 pheric precipitates or ground waters. 271

Here we will focus on application of latex composites 272 containing CoHCF, which is very selective to cesium ions,¹⁶ for 273 fabrication of coatings assuring efficient fixation of cesium on 274

275 contaminated surfaces and preventing its leaching and
276 migration under contact with liquid media. To implement the
277 suggested concept the following main questions will be
278 addressed: (i) which types of functional groups can be used
279 for fixation of CoHCF on the latex surface; (ii) how does the
280 content of latex surface groups effect colloidal stability of the
281 latex/CoHCF composite, (iii) what content of CoHCF in
282 composite is required to provide efficient fixation of cesium
283 after casting latex/CoHCF composite dispersion on contami-
284 nated surface?

285 3.2. Fabrication and Properties of Latex/CoHCF 286 Composites.

To elucidate requirements to latex surface
287 characteristics, which are important for formation of stable
288 composites with CoHCF, a series of carboxylic and amino
289 latexes varying in content of surface functional groups has been
290 synthesized (Table 1).

291 Since colloids of CoHCF have negative electrokinetic
292 potential,⁸ they cannot be bound to carboxylic latexes via
293 electrostatic interactions but can be formed on the latex surface
294 via the “in situ” growth mechanism. At the first stage of this
295 process, Co^{2+} ions bind to the latex carboxylic groups in the pH
296 range of 5.2–5.4, where carboxylic groups are nearly
297 completely ionized (Supporting Information, Figure S3), and
298 formation of cobalt hydroxides is not yet started. At the second
299 stage, addition of $[\text{Fe}(\text{CN})_6]^{4-}$ initiates the formation of
300 insoluble complex of CoHCF and crystal growth from the latex
301 surface, if the content of carboxylic groups is sufficiently high to
302 ensure nanocrystal attachment and stabilization.

303 As a criterion of the latex/CoHCF composite stability, we
304 used the iron content in the top layer of the dispersion, which
305 remained constant, when no phase separation between latex
306 and CoHCF colloids occurred, or decreased, when unstabilized
307 CoHCF precipitated. Figure 2 shows that CoHCF rapidly

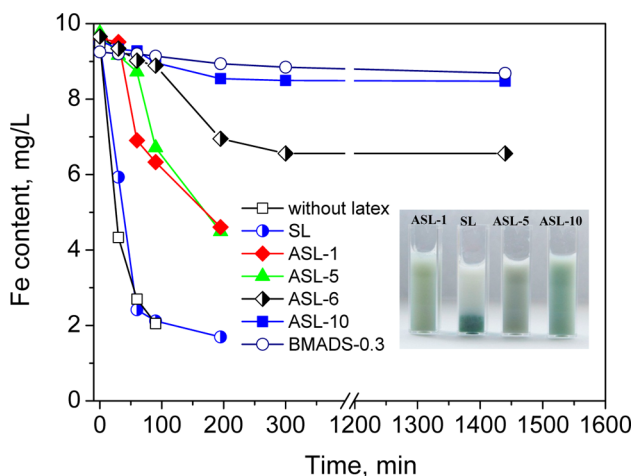


Figure 2. Kinetics of cobalt hexacyanoferrate(II) settling in latex/CoHCF composite dispersions fabricated from latexes with different content of surface functional groups ($\text{pH} = 5.4$, latex solid content 0.5%, CoHCF content 0.035 mmol per 1 g of the latex). Photo of the latex/CoHCF composite dispersions 3 h after fabrication.

308 precipitates in water and in dispersion of SL/CoHCF
309 composite formed with polystyrene latex (SL), which does
310 not contain any ion-exchange sites on the surface. The stability
311 of latex/CoHCF composites significantly increases when
312 carboxylic latexes were used for CoHCF immobilization: the

higher the surface group content was, the better the composite
313 stability was (Figure 2).

Assuming that two carboxylic groups interact with one Co^{2+}
315 ion and cobalt ferrocyanide has the composition close to
316 $\text{Co}_2[\text{Fe}(\text{CN})_6]$, the theoretical capacity of carboxylic latex for
317 $\text{Co}_2[\text{Fe}(\text{CN})_6]$ is 4 times lower than the content of carboxylic
318 groups (Table 1). However, the amount of CoHCF, which can
319 be loaded without loss of composite stability, is noticeably
320 lower than the theoretical latex capacity for CoHCF. For
321 example, up to 0.025 mmol cobalt ferrocyanide can be
322 stabilized in 1 g of latex with the theoretical capacity for
323 CoHCF 0.046 mmol/g (ASL-6). The same tendency was
324 observed for other carboxylic latexes (Supporting Information,
325 Figure S4). This suggests that the distance between surface
326 groups can also play a significant role in attachment of CoHCF
327 to the latex surface. At low content of carboxylic groups and
328 large distance between ion-exchange sites, two adjusting
329 carboxylic groups cannot be involved in stoichiometric surface
330 complexation reactions with one Co^{2+} ion, so the attachment of
331 CoHCF nanocrystals to the latex surface is relatively weak. The
332 most stable composites were obtained when the content of
333 carboxylic groups was at least 5 times higher than theoretically
334 required for CoHCF binding. The most stable composites were
335 obtained for the latex ASL-10 with the carboxylic groups
336 content 1.44 mmol/g.

Only moderate changes in electrokintetic potential of
338 composites were detected with the increase of CoHCF content
339 (Figure 3), since the decrease of carboxylic groups surface
340 f3 charge due to the Co^{2+} ions binding is compensated by
341 subsequent formation of negatively charged CoHCF colloids.
342 The size of composites significantly increases only for ASL-10
343 latex with the highest content of carboxylic groups. The
344 invariable size of all other composites can be attributed either
345 to formation of very small ferrocyanide nanocrystals on the
346 latex surface, so that the composite sizes remain within the
347 experimental error of dynamic light scattering (~10%), or to
348 coexistence of free latex particles and CoHCF colloids.
349

TEM images of composites confirm (Figure 4) that
350 f4 polystyrene latex (SL) and latex with low content of carboxylic
351 groups (ASL-1) do not form composites with CoHCF. Primary
352 particles of CoHCF in these dispersions have the size ~20 nm
353 and are not attached to the latex surface. Thus, composites SL/
354 CoHCF and ASL-1/CoHCF can be considered only as
355 mixtures of two types of particles. CoHCF particles in these
356 dispersions form a continuous network (Figure 4A,B) that
357 results in fast phase separation in composite and CoHCF
358 precipitation, as observed in Figure 2. Structure of ASL-10/
359 CoHCF composite is completely different (Figure 4C): one
360 observes neither primary CoHCF particles nor free latex
361 particles. The composite contains only irregularly shaped
362 particles with the size slightly larger than that of the latex.
363 High-resolution TEM images show that shape irregularity
364 results from formation of CoHCF layer around the latex
365 particles that proves formation of ASL-10/CoHCF composite.
366 Such composites containing up to 0.07 mmol of CoHCF per 1
367 g of latex remain stable at least over 4 months.
368

CoHCF can be also stabilized in dispersions of amino latexes
369 (BMADS-0.3, Figure 2). Since $[\text{Fe}(\text{CN})_6]^{4-}$ ions efficiently
370 interact with aminopolymers,²⁰ an anion-exchange reaction can
371 be used to initiate subsequent *in situ* growth of CoHCF crystals
372 upon Co^{2+} addition. In contrast to carboxylic latexes, negative
373 charge of CoHCF colloids compensates positive charge of the
374 latex surface and composite loses stability at a certain content of
375

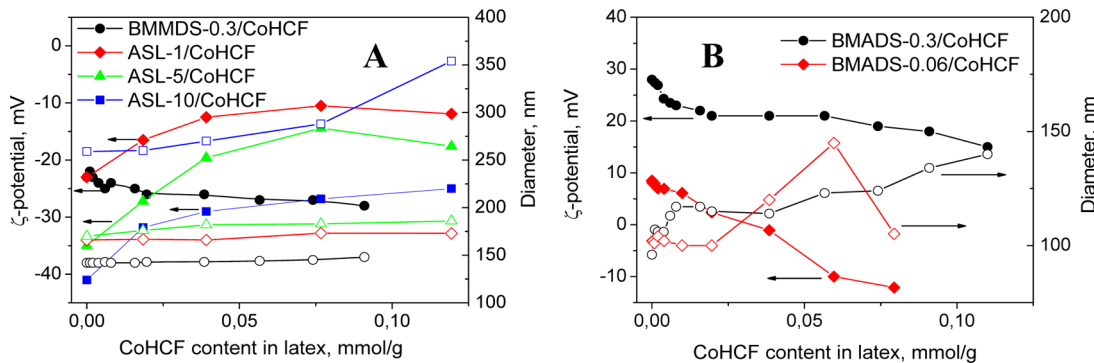


Figure 3. Electrokinetic potentials and particle sizes of carboxylic (A) and amino (B) latex/CoHFC composites ($\text{pH} = 5.4$, 0.001 M KCl). Closed symbols: ζ -potential, open symbols: diameter.

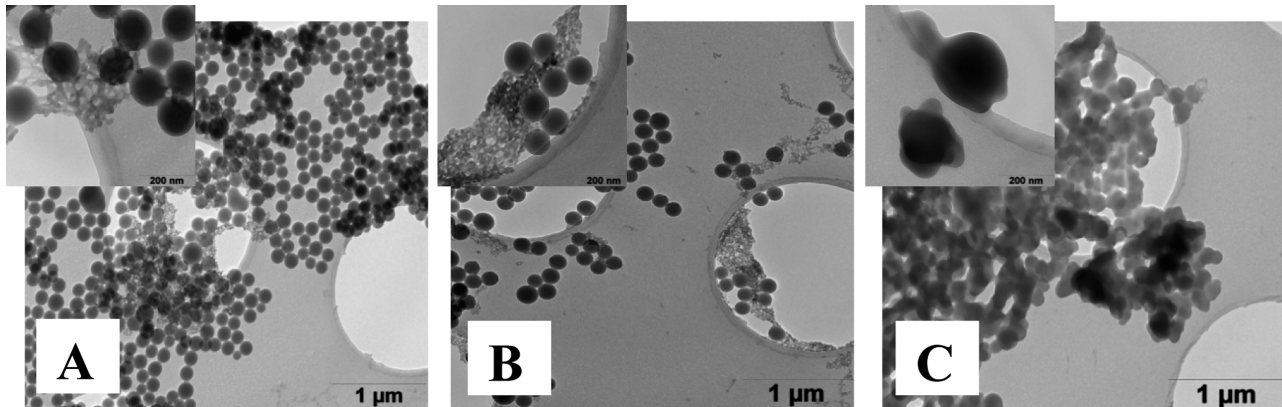


Figure 4. TEM images of latex/CoHFC composites containing 0.035 mmol $\text{Co}_2[\text{Fe}(\text{CN})_6]$ per 1 g of the latex: SL (A), ASL-1 (B), ASL-10 (C).

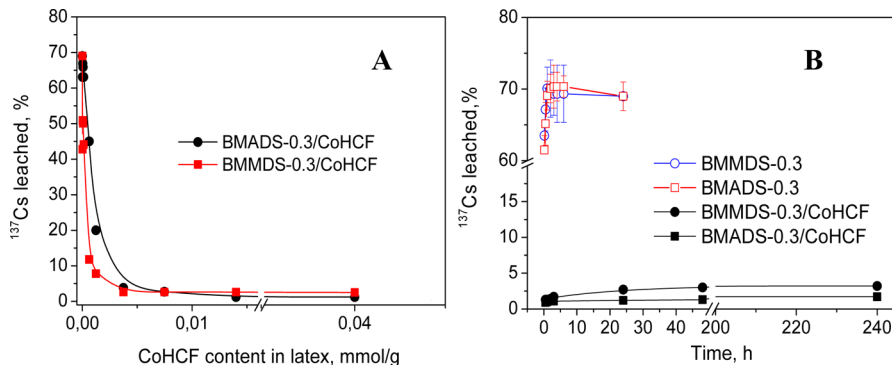


Figure 5. ^{137}Cs leaching with water from contaminated sand surface coated with latex/CoHCF composites varying in CoHCF content (A). Kinetics of ^{137}Cs leaching from contaminated sand surface coated with original latexes and latex/CoHCF composites containing 0.035 mmol CoHCF per 1 g of latex (B).

376 CoHCF. Because of the charge reversal, composites based on
377 latex BMADS-0.06 with low content of amino groups are
378 unstable at a CoHCF content of 0.025–0.06 mmol per 1 g of
379 latex (Figure 3B, Supporting Information, Figure S5), while
380 BMADS-0.3/CoHCF composite remained stable even when
381 CoHCF content was increased to 0.11 mmol per 1 g of the
382 latex.

383 **3.3. Fabrication and Properties of Latex/CoHCF**
384 **Composite Coatings.** In contrast to polystyrene-based
385 latexes, which are not film-forming, copolymers of acrylics
386 and styrene with siloxanes and silanes are widely used in
387 protective coatings due to their enhanced adhesion to the
388 surface and water repellence.^{21,22} In the present work, latex/
389 CoHCF composites applicable for formation of dust-suppress-

390 ing coatings were fabricated using a series of copolymer latexes 391 consisting of butyl acrylate, methyl methacrylate, diethoxy- 392 (methyl)vinyl silane, and different concentrations of methacrylic 393 acid or aminoethyl methacrylate units (Table 1). Here, we were 394 aimed to find an optimum content of the selective sorbent in 395 the latex/CoHCF composite to be used for fabrication of 396 coatings preventing cesium migration with liquid media from 397 ^{137}Cs -contaminated surface. This experiment simulates the 398 behavior of dust suppressor films in open air under the effects 399 of atmospheric precipitates and groundwater leaching. 399

To account for the effect of the latex type, composites were 400 prepared using amino latex BMADS-0.3 and carboxylic latex 401 BMMDS-0.3. Both BMMDS-0.3 and BMADS-0.3 original 402

Table 2. Effect of Latex/CoHCF Composite Coatings Characteristics on ^{137}Cs Leaching from Contaminated Sand

	latex	latex solid content, %	thickness, μm^a	CoHCF volume fraction, ^b %	leaching media	^{137}Cs leached, % ^c
1	BMMDS-0.3	2	2.95	0.63	water	5.0 \pm 0.5
2		2		0.63	0.1 M NaCl	5.6 \pm 0.5
3		2		0.63	0.5 M NaCl	10.4 \pm 1
4		5	5.63	2.06	water	0.9 \pm 0.2
5		10	27.03	1.72	water	0.5 \pm 0.2
6	BMADS-0.3	2	4.03	0.46	water	1.2 \pm 0.2
7		2		0.46	0.1 M NaCl	3.0 \pm 0.3
8		2		0.46	0.5 M NaCl	4.8 \pm 0.5
9		5	5.74	2.02	water	1.0 \pm 0.2
10		10	29.53	1.57	water	0.4 \pm 0.2

^aFilm thickness was calculated from cross-section SEM images. ^bThe CoHCF content in composites is fixed to 0.014 mmol per 1 g of latex.

^cLeached with water after 24 h.

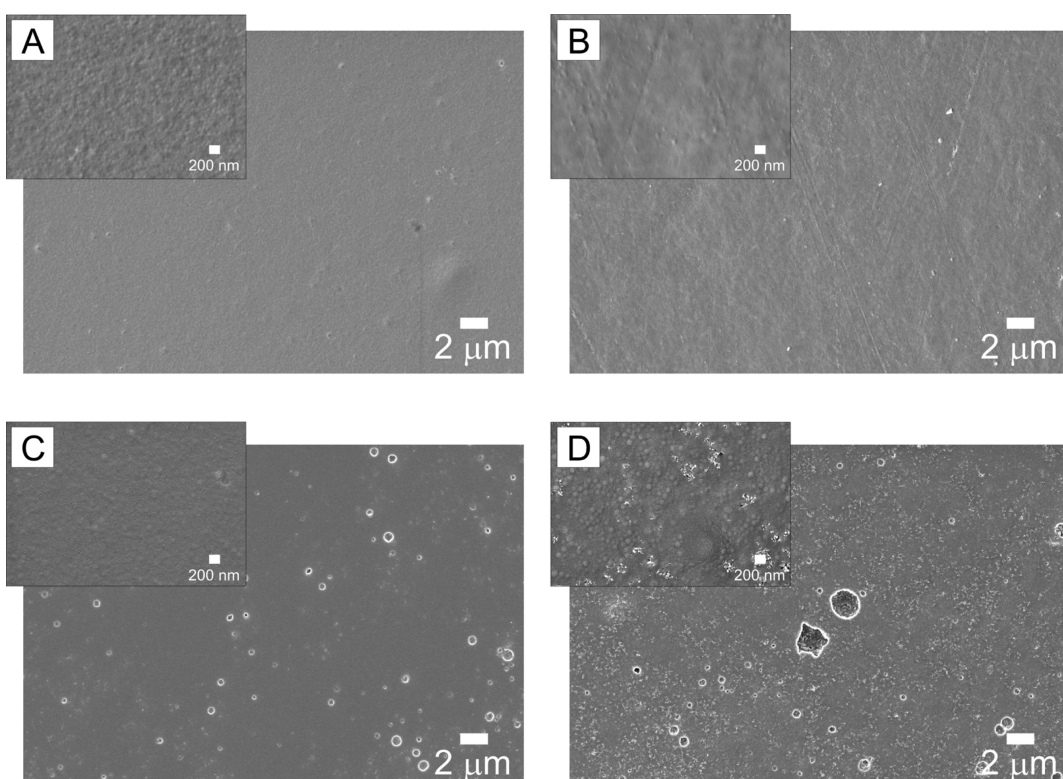


Figure 6. SEM images of coatings casted from 2% latex dispersions on silicon wafers: BMMDS-0.3 (A), BMADS-0.3 (B), BMMDS-0.3/CoHCF (C), BMADS-0.3/CoHCF (D). CoHCF content in all composites was 0.035 mmol per 1 g of latex.

403 latexes give hydrophilic coatings (advancing contact angles
404 (θ_{adv}) = 59° and 54° , respectively), which are highly
405 permeable for ^{137}Cs radionuclides. Investigations of the ^{137}Cs -
406 leaching kinetics (Figure 5) revealed fast migration of 70% of
407 cesium from the quartz sand surface within 30 min of contact.
408 However, ^{137}Cs leaching was reduced to 0.4–2.5% when
409 composite latex/CoHCF coatings were formed on contami-
410 nated surface before it was brought to contact with water
411 (Figure 5A). Figure 5A shows that CoHCF content in the
412 composites used for coating formation can be as low as ~ 0.01
413 mmol/g. Despite the latex coatings hydrophilicity, 10 d of
414 monitoring the ^{137}Cs leaching showed only slight increase of
415 ^{137}Cs content in liquid media indicating long-term stability of
416 the composite coatings (Figure 5B).

417 At the same content of CoHCF in latex/CoHCF composites
418 (0.014 mmol CoHCF per 1 g of latex, latex solid content 2%),
419 the efficiency of coatings in ^{137}Cs fixation was higher for

420 BMADS-0.3-based composite that correlates with the coatings 420
421 thickness (Table 2). Although the volume fraction of the 421 t2
422 sorbent (CoHCF) is lower in thicker BMADS-0.3/CoHCF 422
423 composite coating, the longer ionic pathway is, most likely, 423
424 beneficial to minimize cesium leaching caused by the coating 424
425 defects.

426 SEM images of the latex coatings and composite coatings 426
427 demonstrate a significant difference in their surface topography 427
428 (Figure 6). Hybrid coatings formed by BMMDS-0.3 and 428 f6
429 BMADS-0.3 latexes are rougher than original latex coatings and 429
430 exhibit small hole defects, which can originate from the high 430
431 interfacial tension between polymer and inorganic nano- 431
432 particles. Note that we were not aimed here to optimize film 432
433 forming properties of the latexes, so no coalescing aids were 433
434 added to avoid any interference with composite formation that 434
435 could complicate data interpretation. SEM images also show 435
436 that distribution of CoHCF nanoparticles in dry composite 436

437 coatings is not perfectly homogeneous (Figure 6) but their
438 crystal size remains in nanoscale range. XRD patterns of
439 coatings exhibit only weak reflections of CoHCF typical for
440 nanosized crystals (Supporting Information, Figure S6).

441 According to the data shown in Table 2 (lines 4, 5, 9, 10),
442 ^{137}Cs leaching can be minimized by increasing thickness
443 BMMDS-0.3 and BMADS-0.3 composite coatings. The films
444 cast from composite dispersions with latex solid contents of 5%
445 and 10% and fixed CoHCF content per 1 g of latex showed
446 significantly lower rate of ^{137}Cs leaching. Thus, both latex
447 types—containing carboxylic and amino groups—can be used
448 for fabrication of composite coatings for cesium fixation.

449 The important issue for environmental applications of such
450 composite coatings is their performance in the presence of
451 other cations. Transition metal hexacyanoferrates (II) are very
452 selective to cesium ions but sensitive to the presence of sodium
453 and potassium ions at high concentrations.¹⁷ We have
454 previously shown that ^{137}Cs distribution coefficients for latex/
455 CoHCF composites in dispersions remained sufficiently high
456 even in 2 M NaCl solution, while ^{137}Cs distribution coefficients
457 for composite materials obtained by electrochemical deposition
458 of latex/CoHCF on carbon fibers dropped significantly already
459 in 0.1 M NaCl solution.⁸ The most probable reason for this
460 effect is the difference in sodium ion concentration inside and
461 outside latex film due to the existence of the Donnan potential.
462 Since this effect is more pronounced for cation-exchangers
463 (carboxylic latexes), migration of ^{137}Cs from BMMDS-0.3/
464 CoHCF composite coatings to liquid media increases from
465 5.6% in 0.1 M NaCl to ~10% in 0.5 M NaCl within 24 h
466 (Table 2, lines 2–3, 7–8). However, the concentration of
467 sodium ions in the environment (in soil and ground waters),
468 aside from sea-coastal areas, is substantially lower than 0.1 M,
469 and, thus, shall not significantly decrease efficiency of latex/
470 CoHCF composite coatings.

4. CONCLUSIONS

471 Preventing migration of radionuclides from contaminated solid
472 surfaces into environment after nuclear accidents remains a
473 challenging task. Application of polymeric dust suppressors
474 helps to securely eliminate migration of radionuclides with
475 aerosols but does not limit their mobility under contact with
476 atmospheric precipitates, ground, and soil waters due to
477 solubility and/or permeability of polymeric fixatives. Thus,
478 long-term open-air application of conventional fixatives is
479 associated with radionuclide migration from soil surface
480 downward into the soil profile that significantly increase
481 volume of soil, which must be removed or decontaminated.
482 Here we have presented a new concept to form composite
483 fixative coatings on radioactively contaminated surfaces, which,
484 due to combination of dust-suppressing properties of film-
485 forming latexes and selective sorption properties of nanosized
486 sorbents, can eliminate migration of radionuclides with both
487 aerosols and surface and ground waters.

488 Here we have demonstrated fabrication of composite
489 coatings for fixation of cesium radionuclides using colloidal
490 stable latex/cobalt hexacyanoferrate(II) (CoHCF). A series of
491 latex/CoHCF containing amino and carboxylic functional
492 groups has been synthesized and used for latex/CoHCF
493 composites fabrication. We have shown that the optimal
494 concentration of $-\text{COOH}$ groups on the surface of carboxylic
495 latexes for latex/CoHCF fabrication is close to 1 mmol per 1 g
496 of latex, while amino-latexes containing only 0.1 mmol $-\text{NH}_2$

497 groups per 1 g of latex can be used due to the electrostatic
498 contribution to composite stabilization in the latter case.

499 Composite coatings for cesium fixation have been fabricated
500 on ^{137}Cs -contaminated sand by casting colloidal stable latex/
501 CoHCF composites with various CoHCF contents. After
502 exposure of contaminated sand it was found that ^{137}Cs leaching
503 with water from contaminated sand coated with latex/CoHCF
504 composites can be reduced to 0.4%, whereas coatings formed
505 by original latexes allows fast migration of 70% of cesium from
506 the surface within 30 min. ^{137}Cs migration from the surface was
507 efficiently eliminated when the latex/CoHCF composites
508 containing only ~0.01 mmol CoHCF per 1 g of latex were
509 used. 10 d of monitoring the ^{137}Cs leaching has shown only
510 slight increase of the cesium content in liquid media indicating
511 long-term stability of the composite coatings.

512 An important advantage of such approach consists in the
513 possibility to use commercially available dust-suppressors,
514 which are mainly carboxylic latexes, and modify their properties
515 by addition of relatively low amount of selective inorganic
516 materials, which does not significantly increase production costs
517 but opens a window for fabrication of coatings for entrapment
518 of a wide range of target radionuclides, if appropriate nanosized
519 selective sorbents are used.

■ ASSOCIATED CONTENT

Supporting Information

520 Compositions of the reaction mixture used for latex synthesis
521 (Table S1), electrokinetic properties of latexes (ζ -potential vs
522 pH); size distributions and DLS correlation functions for
523 original latexes and latex/CoHCF composites, kinetics of cobalt
524 hexacyanoferrate(II) settling in amino latex/CoHCF composite
525 dispersions and carboxylic latex/CoHCF composites with
526 different CoHCF content;; XRD patterns of latex/CoHCF
527 composites (Figures S1–S6). This material is available free of
528 charge via the Internet at <http://pubs.acs.org>.

■ AUTHOR INFORMATION

Corresponding Author

532 *Telephone: +7-423-2311889. E-mail: sbratska@ich.dvo.ru.

Author Contributions

533 The manuscript was written through contributions of all
534 authors. All authors have given approval to the final version of
535 the manuscript.

Notes

536 The authors declare no competing financial interest.

■ ACKNOWLEDGMENTS

541 The work was done with financial support from the seventh EU
542 Research Framework Programme for ERANET-Russia project
543 (STProject No. 144). Assistance of L. Schellkopf (Leibniz-
544 Institut für Polymerforschung Dresden e.V) in acquiring TEM
545 images is gratefully acknowledged.

■ REFERENCES

- (1) Zengeni, E.; Hartmann, P. C.; Pasch, H. Encapsulation of Clay by Ad-Miniemulsion Polymerization: The Influence of Clay Size and Modifier Reactivity on Latex Morphology and Physical Properties. *ACS Appl. Mater. Interfaces* **2012**, *4*, 6956–6967.
- (2) Wen, N.; Tang, Q.; Chena, M.; Wu, L. Synthesis of PVAc/SiO₂ Latices Stabilized by Silica Nanoparticles. *J. Colloid Interface Sci.* **2008**, *320*, 152–158.

- 554 (3) Watanabe, M.; Minami, Y.; Masuyama, A.; Matsukawa, K. Hybrid
555 Films Prepared from Latex Particles Incorporating Metal Oxide
556 Nanoparticles. *Res. Chem. Intermed.* **2013**, *39*, 291–300.
- 557 (4) Liu, W. J.; He, W. D.; Wang, Y. M.; Wang, D.; Zhang, Z. C. New
558 Approach to Hybrid Materials: Functional Sub-micrometer Core/shell
559 Particles Coated with NiS Clusters by γ -irradiation. *Polymer* **2005**, *46*,
560 8366–8372.
- 561 (5) Wada, T.; Uragami, T. Preparation and Characteristics of a
562 Waterborne Preventive Stain Coating Material with Organic-Inorganic
563 Composites. *JCT Res.* **2006**, *3*, 267–274.
- 564 (6) Zhou, X. D.; Chen, F.; Yang, J. T.; Yan, X. H.; Zhong, M. Q.
565 Preparation and Self-Sterilizing Properties of Ag@TiO₂–Styrene–
566 Acrylic Complex Coatings. *Mater. Sci. Eng.* **2013**, *C 33*, 1209–1213.
- 567 (7) Surbeck, H. Alpha Spectrometry Sample Preparation using
568 Selectively Adsorbing thin Films. *Appl. Radiat. Isot.* **2000**, *53*, 97–100.
- 569 (8) Avramenko, V.; Bratskaya, S.; Zhelezov, V.; Sheveleva, I.;
570 Voitenko, O.; Sergienko, V. Colloid Stable Sorbents for Cesium
571 Removal: Preparation and Application of Latex Particles Function-
572 alized with Transition Metals Ferrocyanides. *J. Hazard. Mater.* **2011**,
573 *186*, 1343–1350.
- 574 (9) Parra, R. R.; Medina, V. F.; Conca, J. L. The Use of Fixatives for
575 Response to a Radiation Dispersal Devise Attack - a Review of the
576 Current (2009) State-of-the-Art. *J. Environ. Radioact.* **2009**, *100*, 923–
577 934.
- 578 (10) Andersson, K. G.; Roed, J. Removal of Radioactive Fallout from
579 Surface of Soil and Grassed Surfaces using Peelable Coatings. *J.
580 Environ. Radioact.* **1994**, *22*, 197–203.
- 581 (11) Klyuchnikov, A. A.; Krasnov, V. A.; Rud'ko, V. M.; Shcherbin, V.
582 N. Ob'ekt "Ukrytie" 1986–2006 ("Shelter" 1986–2006): Chernobyl.
583 *IPB AES NAN Ukraina* **2006**, 168.
- 584 (12) Nakano, M.; Yong, R. N. Overview of Rehabilitation Schemes
585 for Farmlands Contaminated with Radioactive Cesium Released from
586 Fukushima Power Plant. *Eng. Geol. (Amsterdam, Neth.)* **2013**, *155*, 87–
587 93.
- 588 (13) Fujiwara, T.; Saito, T.; Muroya, Y.; Sawahata, H.; Yamashita, Y.;
589 Nagasaki, S.; Okamoto, K.; Takahashi, H.; Uesaka, M.; Katsumura, Y.;
590 Tanaka, S. Isotopic Ratio and Vertical Distribution of Radionuclides in
591 Soil Affected by the Accident of Fukushima Dai-ichi Nuclear Power
592 Plants. *J. Environ. Radioact.* **2012**, *113*, 37–44.
- 593 (14) *Handbook of Parameter Values for the Prediction of Radionuclide
594 Transfer Terrestrial and Freshwater Environments*; Technical Reports
595 Series 472; IAEA: Vienna, Austria, 2010.
- 596 (15) Shand, C. A.; Rosén, K.; Thored, K.; Wendler, R.; Hillier, S.
597 Downward Migration of Radio caesium in Organic Soils Across a
598 Transect in Scotland. *J. Environ. Radioact.* **2013**, *115*, 124–133.
- 599 (16) Andersson, K. *The Characterization and Removal of Chernobyl
600 Debris in Garden Soils*; Riso-M-2912: Riso Library, Riso National
601 Laboratory: Roskilde, Denmark, 1991.
- 602 (17) Haas, P. A. A Review of Information on Ferrocyanide Solids for
603 Removal of Cesium from Solutions. *Sep. Sci. Technol.* **1993**, *28*, 2479–
604 2506.
- 605 (18) Musyanovich, A.; Rossmanith, R.; Tontsch, C.; Landfester, K.
606 Effect of Hydrophilic Comonomer and Surfactant Type on the
607 Colloidal Stability and Size Distribution of Carboxyl- and Amino-
608 Functionalized Polystyrene Particles Prepared by Miniemulsion
609 Polymerization. *Langmuir* **2007**, *23*, 5367–5376.
- 610 (19) Jansat, S.; Pelzer, K.; Garcia-Anton, J.; Raucoules, R.; Philippot,
611 K.; Maisonnat, A.; Chaudret, B.; Guari, Y.; Mehdi, A.; Reye, C.; Corriu,
612 R.J. R. Synthesis of New RuO₂@SiO₂ Composite Nanomaterials and
613 their Application as Catalytic Filters for Selective Gas Detection. *Adv.
614 Funct. Mater.* **2007**, *17*, 3339–3347.
- 615 (20) Khutoryanskiy, V. V.; Nurkeeva, Z. S.; Mun, G. A.; Sergaziyev,
616 A. D.; Kadlubowski, S.; Fefelova, N. A.; Baizhumanova, T.; Rosiak, J.
617 M. Temperature-Responsive Linear Polyelectrolytes and Hydrogels
618 Based on [2-(methacryloyloxy)ethyl] trimethylammonium chloride
619 and N-isopropylacrylamide and Their Complex Formation with
620 Potassium Hexacyanoferrates (II, III). *J. Polym. Sci., Part B: Polym.
621 Phys.* **2004**, *42*, 515–522.
- 621 (21) Watanabe, M.; Toshiyuki, T. Acrylic Polymer/Silica Organic-
622 Inorganic Hybrid Emulsions for Coating Materials: Role of the Silane
623 Coupling Agent. *J. Polym. Sci., Part A: Polym. Chem.* **2006**, *44*, 4736–
624 4742.
- 625 (22) Zou, M. X.; Wang, S. J.; Zhang, Z. C.; Ge, X. W. Preparation
626 and Characterization of Polysiloxane-poly(butyl acrylate-styrene)
627 Composite Latices and Their Film Properties. *Eur. Polym. J.* **2005**, *41*,
628 2602–2613.
- 629